WHIRL AND WHIP - ROTOR/BEARING STABILITY PROBLEMS

Agnes Muszynska
Bently Rotor Dynamics Research Corporation
Minden, Nevada 89423

A mathematical model of a symmetric rotor supported by one rigid and one fluid lubricated bearing is proposed in this paper. The rotor model is represented by generalized (modal) parameters of its first bending mode. The rotational character of the bearing fluid force is taken into account. The model yields synchronous vibrations due to rotor unbalance as a particular solution of the equations of motion, rotor/bearing system natural frequencies and corresponding self-excited vibrations known as "oil whirl" and "oil whip." The stability analysis yields rotative speed threshold of stability. The model also gives the evaluation of stability of the rotor synchronous vibrations. In the first balance resonance speed region two more thresholds of stability are yielded. The width of this stability region is directly related to the amount of rotor unbalance.

The results of the analysis based on this model stand with very good agreement with field observations of rotor dynamic behavior and the experimental results.

1. INTRODUCTION

Dynamic phenomena induced by interaction between the rotor and bearing or seal fluid motion and creating severe rotor vibrations have been recognized for over 50 years. High amplitude shaft vibrations which can sustain over a wide range of rotational speeds not only perturb the normal operation of a rotating machine, but may also cause serious damage to the machine and the entire plant.

Literature related to rotor/bearing and rotor/seal phenomena is very rich [1-7]. Availability of computers and fast development of numerical methods are bringing more and more results based on analytical models of the solid/fluid interaction phenomena.

There is still, however, a big gap between theory and practice.

Practical rotating machinery instability problems in the field are being corrected ad hoc by applying trial and error approach with a number of measures such as increasing rotor radial load, modifying lubricant temperature and/or pressure, shortening and stiffening the shaft, or replacing bearings or seals with "more stable" ones. However, the only measure which corrects the causative agent is the recently introduced anti-swirling technique.

Researchers and engineers do not always agree upon the physical description of the shaft/bearing or shaft/seal solid/fluid interaction dynamic phenomena. The complex-

ity of these phenomena and the long list of factors affecting them make the picture tremendously obscure.

Most often bearing and/or seal fluid forces generated during rotating machine operation are considered separately from the shaft motion, assuming only that the shaft rotates with constant angular velocity and has a perfect geometry.

Practically observed phenomena indicate that this approach can be justified only for specific conditions, in particular, for low values of shaft rotative speed. In most other cases, rotor and bearings (or rotor/bearings/seals) should be considered as a system. The dynamic behavior of this system will then reflect the rotor/bearing coupled system features.

In this paper, an attempt to build a simple rotor/bearing system model is made. The simplicity allows for obtaining analytical solutions and yields clear conclusions on how various parameters of the rotor/bearing system affect its dynamic behavior. The model is based on modal behavior of the rotor. The model of bearing fluid dynamic forces is developed through a classical approach applied to nonconservative mechanical systems [8].

The model yields results which are in perfect agreement with the observed dynamic phenomena of the rotor/bearing system.

2. OBSERVED VIBRATIONAL PHENOMENA

Lightly loaded and slightly unbalanced symmetrical rotors rotating in fluid 360° lubricated cylindrical bearings, exhibit the following dynamic phenomena:

(i) When the shaft starts rotating with a slowly increasing rotative speed, SYNCHRONOUS (1×) lateral vibrations with minor amplitudes are observed all along the rotor axis. These vibrations are caused by the inertia forces of unbalance of the rotor. At low rotative speeds, these vibrations are stable, an impulse perturbation of the rotor causes a short time transient vibration process, and the same vibration pattern is reestablished (Fig. 1).

(ii) At higher rotational speeds (usually below the first balance resonance), the forced synchronous vibration is not the only regime of vibration. Along with 1× vibrations, OIL WHIRL appears. Oil whirl is the rotor lateral forward precessional subharmonic vibration around the bearing center at a frequency close to half the rotative speed. In this range of the rotative speed, the rotor behaves as a rigid body. The amplitudes of oil whirl are usually much higher than those of synchronous vibrations; they are, however, limited by the bearing clearance and the fluid nonlinear forces. With increasing rotative speed, the pattern of vibration remains stable. The oil whirl "half" frequency follows the increasing rotative speed, maintaining the ≈1/2 ratio with it. The vibration amplitudes remain nearly constant and usually high. At the bearing, the vibration amplitude may cover nearly all bearing clearance. In the considered range of rotative speed, the bearing fluid dynamic effects clearly dominate. The forced synchronous vibration represents a small fraction of vibration response, as the spectrum indicates (Fig. 1).

(iii) When the increasing rotative speed approaches the first balance resonance, i.e., the first natural frequency of the rotor, oil whirl suddenly becomes unstable and disappears, being suppressed and replaced by increasing SYNCHRONOUS vibrations. The forced vibrations dominate, reaching the highest amplitudes at resonant frequency corresponding to the mass/stiffness/damping properties of the rotor. The bearing fluid dynamic effects now yield priority to the elastic rotor mechanical effects.

(iv) Above the first balance resonance speed, the synchronous forced vibrations decay. Again, the bearing-fluid forces come back into action. With increasing rotative speed, shortly after the first balance resonance, OIL WHIRL occurs again. The previously described pattern repeats. The width of the rotative speed region in which the synchronous vibration dominate depends directly on the amount of rotor unbalance: higher unbalance, wider is this region.

(v) When the rotative speed approaches double the value of the rotor first balance resonance, the half-speed oil whirl frequency reaches the value of the first balance resonance -- the first natural frequency of the rotor. The oil whirl pattern is replaced by OIL WHIP -- a lateral forward precessional subharmonic vibration of the rotor. Oil whip has a constant frequency: independently of the rotative speed increase, the oil whip frequency remains close to the first natural frequency of the rotor. In this range of high rotative speed, the shaft cannot be considered rigid. Its flexibility, i.e., additional degrees of freedom, causes that rotor/bearing system is closely coupled. The rotor parameters (its mass and stiffness, in particular) become the dominant dynamic factors. The amplitude of oil-whip journal vibration is limited by the bearing clearance, but the shaft vibration may become very high, as the shaft vibrates at its natural frequency, i.e., in the resonant conditions.

In various machines furnished with fluid lubricated bearings and/or seals, the above-described phenomena may take various forms, as other external factors may affect the system dynamic behavior. Generally, however, similar patterns can be expected [9].

Among the described dynamic phenomena, there is a clear distinction related to their nature: (a) rotor synchronous lateral vibration (1×) due to unbalance and (b) rotor fluid-related vibration. The first type is typically forced vibration. The rotating periodic inertia force considered "external" to rotor lateral motion causes the rotor response with the same frequency. The resulting motion has the form of the classical synchronous (1×) excited vibration.

As there is no other external force to excite the vibrations, it is quite reasonable to refer to the second type of vibration, as SELF-EXCITED vibrations, occurring due to an internal feedback mechanism transferring the rotative energy into vibrations. Self-excited vibrations cannot occur in a conservative or "passive" structure, with no energy supply (in nonrotating systems in particular). In passive structures, the free vibrations following an external perturbing impulse usually have a decaying character, due to the stabilizing effect of damping, naturally existing in the system. Another situation takes place if the system is subject to a constant supply of energy (an "active", nonconservative structure). Well recognized are wind induced vibrations known as flutter. The rotating machine belongs also to this category. The internal energy transfer mechanism, in this case a bearing fluid involvement in motion, uses a part of the rotative energy to create forces, having the direction opposite to the damping force. The result consists of reduction, then with their

increasing value, a nullification of effective damping, the stabilizing factor. In such conditions, free vibrations do not have the decaying character anymore (effect of negative damping). While vibration amplitude increases, nonlinear factors become significant and eventually amplitudes are limited. Vibrations become periodic with a constant amplitude. The stable limit cycle is reached. This represents the practically observed case of the oil whirl and oil whip. As the oil whirl and oil whip occur in the system having a constant energy supply, the resulting vibration is referred to as self-excited. The last term is also closely related to the nonlinear character of the phenomena. In particular, the size of the oil whirl/whip orbits (limit cycle vibration amplitudes) are determined exclusively by the nonlinear factors in the oil bearing.

Simple linear modelization of the rotor/bearing system can be applied as a first approximation in mathematical description of the observed phenomena. The linear model provides the spectrum of natural frequencies of the system, as these frequencies are very insensitive to nonlinear factors. The linear model also gives the evaluation of stability threshold, closely related to the delicate balance between the system's natural damping and the bearing fluid forces acting in antiphase and opposing damping.

Very often oil whirl and oil whip are described as "unstable" rotor motion in a sense which is rather close to the terms "undesirable" or "unacceptable" rotor vibrations. Obviously, oil whirl/whip vibrations are highly undesirable; they disturb the machine's normal operation. The "normal operation" is related to the pure rotational motion of the rotor, around the proper axis and following a suitable angular speed. This is the only regime of motion which is required. The occurrence of the oil whirl/whip vibrations signifies that this pure rotational regime becomes UNSTABLE*, and the oil whirl/whip vibrations represent a STABLE regime. The term "stability" is used here in the most popular sense (following Lyapunov's definition). The pure rotational motion (meaning zero lateral vibration) is unstable, oil whirl/whip lateral vibrations are stable. They exist, and any impulse perturbation cannot significantly modify their pattern. After a short-time transient process, the oil whirl/whip pattern is reestablished.

A practical stability definition for a rotating machine is discussed in [10].

3. FLUID FORCES

Derivation of fluid forces in a bearing (or a seal) is based on the consideration that the fluid rotation (dragged into motion by shaft rotation) plays an appreciable role in resulting dynamic phenomena and may, therefore, have a significant effect on rotor vibrations [8, 11, 12].

In the following presentation, an assessment of this effect is attempted in simplified terms. It is assumed that when the shaft is rotating centered, fully developed fluid flow is established in the circumferential direction, that is, on the average, the fluid is rotating at the rate $\lambda\omega_R$ where ω_R is the shaft rotative speed and λ is the fluid average swirling ratio which value is close to a half (Fig. 2). It is

* Actually, with existing residual imbalance, the rotor pure rotational motion of a rotor does not exist. The only regime is forced synchronous lateral vibration along with the rotation. "Stability" refers then to the stability of this regime.

supposed that shaft lateral vibrations are small enough to make modifications of this pattern negligible. The flow axial component is supposed to affect values of the fluid forces in the x,y plane in a parametric way only, i.e., the fluid circumferential force may proportionally increase with increasing axial flow. However, it is assumed that there is no feedback, i.e., the fluid axial motion is uncoupled from the circumferential motion (and not investigated in this paper). It is also assumed that the axial flow does not modify the average swirling ratio λ.

The vital assumption is that the fluid force which results from averaging the circumferential flow is rotating with angular velocity $\lambda\omega_R$. In rotating reference coordinates x_r, y_r (Fig. 2), the average fluid flow is purely rectilinear and the fluid force is as follows:

$$F = [K_0+\psi_1(|z_r|)]\, z_r + [D+\psi_2(|z_r|)]\, \dot{z}_r + M_f \ddot{z}_r \qquad (1)$$

where $z_r = x_r + jy_r$ $\qquad j = \sqrt{-1}$ $\qquad |z_r| = \sqrt{x_r^2+y_r^2}$

In the equation (1) K_0, D, and M_f are fluid stiffness, damping and inertia coefficients respectively. ψ_1 and ψ_2 are nonlinear functions of the radial displacement $|z_r|$. It is assumed that these functions have analytical character (or at least are continuous, with continuous first two derivatives). Later on, as an example, the following nonlinear functions will be analyzed (the first symmetric term of the Taylor series for any nonlinear analytical function):

$$\psi_{1,2} = B_{1,2}|z_r|^2 \ , \qquad (2)$$

where B_1 and B_2 are positive constants.

The average fluid force (1) has, therefore, nonlinear character. Stiffness and damping components of the fluid force increase with increasing journal eccentricity.

In fixed reference coordinates x,y (Fig. 2), the fluid force will have the following form:

$$F = [K_0+\psi_1(|z|)]\, z + [D+\psi_2(|z|)]\, (\dot{z}-j\lambda\omega_R z) + M_f(\ddot{z}-2j\lambda\omega_R\dot{z}-\lambda^2\omega_R^2 z) \qquad (3)$$

where $z = x+jy$, $|z| = \sqrt{x^2+y^2}$. The equation $z = z_r e^{j\lambda\omega_R t}$ represents transformation of coordinates.

The fluid force (3) can be presented in a classical "bearing coefficient" format:

$$\begin{bmatrix} F_x \\ F_y \end{bmatrix} = \begin{bmatrix} M_f & 0 \\ 0 & M_f \end{bmatrix}\begin{bmatrix} \ddot{x} \\ \ddot{y} \end{bmatrix} + \begin{bmatrix} D & 2\lambda\omega_R M_f \\ -2\lambda\omega_R M_f & D \end{bmatrix}\begin{bmatrix} \dot{x} \\ \dot{y} \end{bmatrix} + \begin{bmatrix} K_0-\lambda^2\omega_R^2 M_f & \lambda\omega_R D \\ -\lambda\omega_R D & K_0-\lambda^2\omega_R^2 M_f \end{bmatrix}\begin{bmatrix} x \\ y \end{bmatrix} +$$
$$+ \begin{bmatrix} \psi_2(|z|) & 0 \\ 0 & \psi_2(|z|) \end{bmatrix}\begin{bmatrix} \dot{x} \\ \dot{y} \end{bmatrix} + \begin{bmatrix} \psi_1(|z|) & \lambda\omega_R\psi_2(|z|) \\ -\lambda\omega_R\psi_2(|z|) & \psi_1(|z|) \end{bmatrix}\begin{bmatrix} x \\ y \end{bmatrix}$$

The last two matrices contain nonlinear components of the fluid force. As it is easily noticed, the fluid force is supposed to have a symmetric character: the diagonal terms are identical, the off-diagonal terms are skew symmetric. More important, however, is the fact that the off-diagonal terms are generated as the result

of rotational character of the fluid force: the tangential (or "cross") damping is the result of Coriolis inertia force, the tangential (or "cross") stiffness is generated by the relative velocity and radial damping. In addition, the radial stiffness K_0 appearing at the main diagonal of the stiffness matrix is now modified by the centripetal fluid inertia force which appears with the negative sign.

During experimental testing by applying perturbation method [13], the character of the fluid force expressed by the equation (3) was fully confirmed. For relatively large clearance-to-radius ratio, the fluid inertia force become significant, and modifies "damping" and "stiffness" matrices considerably. The resultive radial stiffness can very easily reach negative values.

Another important conclusion relates to the "cross stiffness" coefficient, the most important component affecting rotor stability. This term is directly generated by the linear radial damping D, as the result of rotating character of the damping force. This term is proportional to the rotative speed ω_R, i.e., its significance increases with rotative speed. An immediate conclusion is that an increase of the bearing damping D will not help to prevent rotor instability as the "cross stiffness" increases proportionally to D. The only help in decreasing the "cross stiffness" term is a modification of the average swirling ratio λ. This feature is now being widely used in "anti-swirling" devices [14, 15].

4. MATHEMATICAL MODEL OF A SYMMETRIC FLEXIBLE SHAFT ROTATING IN ONE RIGID ANTIFRICTION BEARING AND ONE OIL 360° LUBRICATED CYLINDRICAL BEARING

Oil whirl and oil whip phenomena are characterized by low frequency, that is why it seems reasonable to limit the rotor model to its lowest bending mode. It is obvious that the considerations presented below can be applied to more complex rotor model (including more modes, gyroscopic effect, internal damping, etc.) as well.

The mathematical model representing balance of forces in the symmetric rotor shown in Fig. 3 is as follows:

$$M_1\ddot{z}_1 + D_s\dot{z}_1 + (K_1+K_2)z_1 - K_2z_2 = mr\omega_R^2 e^{j\omega_R t} \tag{4}$$

$$M_2\ddot{z}_2 + M_f(\ddot{z}_2 - 2j\lambda\omega_R\dot{z}_2 - \lambda^2\omega_R^2 z_2) + [D+\psi_2(|z_2|)](\dot{z}_2 - j\lambda\omega_R z_2) + [K_0+\psi_1(|z_2|)]z_2 + \tag{5}$$

$$+ K_3z_2 + K_2(z_2-z_1) = 0 \quad , \quad z_1 = x_1 + jy_1 \quad , \quad z_2 = x_2 + jy_2$$

where M_1, M_2 are rotor generalized (modal) masses, D_s is external generalized (viscous) damping coefficient, K_1, K_2, and K_3 are shaft generalized (modal) stiffness coefficients (K_3 may also include an external spring stiffness), m and r are mass and radius of modal unbalance respectively. The bearing fluid dynamic force is introduced to the equation (5) in the form (3).

The equation (4) presents the classical relationship for an unbalanced symmetric rotor at its first bending mode. Any classical method of modal reduction can be applied to obtain the rotor generalized (modal) coefficients. The equation (5) describes balance of forces, including nonlinear fluid force, acting at the journal. Radial forces (such as gravity) are balanced by external spring forces and are not included in the model (4), (5).

5. SYNCHRONOUS SOLUTION: 1× ROTOR FORCED VIBRATIONS DUE TO UNBALANCE

In this section, the particular solution of equations (4) and (5) will be discussed. This solution describes rotor synchronous vibrations due to unbalance force and has the following form:

$$z_1 = A_1 e^{j(\omega_R t+\alpha_1)} \quad , \quad z_2 = A_2 e^{j(\omega_R t+\alpha_2)} \tag{6}$$

where the amplitudes A_1, A_2 and phase angles α_1, α_2 can be found from the following algebraic equations resulting from (4), (5) and (6):

$$\begin{aligned} &(K_1+K_2+D_s j\omega_R-M\omega_R^2)A_1 e^{j\alpha_1} - K_2 A_2 e^{j\alpha_2} = mr\omega_R^2 \\ &\{K_0+K_2+K_3+\psi_1(A_2)+j[D+\psi_2(A_2)]\omega_R(1-\lambda) - M_2\omega_R^2-M_f\omega_R^2(1-\lambda)^2\}A_2 e^{j\alpha_2}-K_2 A_1 e^{j\alpha_1} = 0 \end{aligned} \tag{7}$$

Note that the fluid inertia and radial damping carry coefficents $1-\lambda$, which value is usually slightly higher than 1/2. This signifies that the effective damping is two times and the fluid inertia effect on synchronous vibrations four times, smaller than their actual values.

The equations (7) can be solved for any given nonlinear functions ψ_1, and ψ_2, as their arguments now become equal to A_2, the journal amplitude of synchronous vibrations. When the nonlinear forces are neglected ($\psi_1=\psi_2=0$) the equations (7) yield simple expressions for the amplitudes and phase angles:

$$A_1 = \frac{mr\omega_R^2}{\sqrt{h_4^2+D_s^2\omega_R^2}} \sqrt{1 + \left(\frac{K_2A_2}{mr\omega_R^2}\right)^2 + 2\,\frac{K_2A_2\cos\alpha_2}{mr\omega_R^2}} \quad , \quad A_2 = \frac{K_2 mr\omega_R^2}{\sqrt{h_2^2+h_3^2}} \tag{8}$$

$$\alpha_1 = \arctan\left(-D_s\omega_R/h_4\right) + \arctan\frac{\tan\alpha_2}{1+mr\omega_R^2/(K_2A_2\cos\alpha_2)} \quad , \quad \alpha_2 = \arctan\left(-h_3/h_2\right) \tag{9}$$

or, further

$$A_1 = \frac{mr\omega_R^2}{\sqrt{h_4^2+D_s^2\omega_R^2}} \sqrt{(h_2+K_2^2)^2+h_3^2} \quad , \quad \alpha_1 = \arctan\left(-D_s\omega_R/h_4\right) + \arctan\left[K_2^2 h_3/(h_2^2+h_3^2+K_2h_2)\right] \tag{10}$$

where
$$h_2 = h_4h_5 - DD_s\omega_R^2(1-\lambda)-K_2^2 \quad , \quad h_3 = [h_5D_s+Dh_4(1-\lambda)]\omega_R \tag{11}$$

$$h_4 = K_1+K_2-M\omega_R^2 \quad , \quad h_5 = K_0+K_2+K_3-\omega_R^2[M_2+M_f(1-\lambda)^2] \tag{12}$$

When the nonlinear forces are given in the form (2), then the amplitude A_2 can be found as the solution of the following polynomial equation:

$$A_2^6(h_6^2+h_7^2) + 2A_2^4(h_2h_6+h_3h_7) + A_2^2(h_2^2+h_3^2) - (K_2mr\omega_R^2)^2 = 0 \tag{13}$$

where
$$h_6 = B_1h_4 - \omega_R^2B_2(1-\lambda) \quad , \quad h_7 = \omega_R[B_2(1-\lambda)h_4+B_1D_s] \tag{14}$$

The phase α_2 in this case is slightly modified by the nonlinear force:

$$\alpha_2 = \arctan\left[\frac{A_2^2\omega_R[D_sB_1+(1-\lambda)h_4B_2]+h_3}{A_2^2[\omega_R^2(1-\lambda)D_sB_2-h_4B_1]-h_2}\right] \tag{15}$$

The amplitude A_1, and phase α_1 are given by equations (8) and (9).

The equation (13) can be solved graphically (Fig. 4). The simple graphical method reveals important qualitative features of the nonlinear system. It is possible that three solutions for A_2 are yielded (Fig. 4a). This corresponds to the well known nonlinear case [16]. More probable, however, is that only one solution exists. The nonlinear force causes a reduction of the vibration amplitude A_2. Figure 5 gives some numerical examples of Bodé plots for the rotor synchronous response. An insensitivity of the response to fluid inertia and journal generalized (modal) mass is noted.

6. STABILITY OF THE PURE ROTATIONAL MOTION OF THE SHAFT

To investigate the stability of the pure rotational motion of the shaft, assume that the unbalance force is equal to zero. For the stability analysis, the nonlinear terms in the equation (5) are neglected, as they are small of the second order. Stability of the pure rotational motion of the shaft means stability of the zero solution of the equations (4) and (5) for mr=0, perturbed by small lateral deflections. The eigenvalue problem with the solution for linearized equations (4), (5) of the form

$$z_1 = E_1 e^{st} \quad , \quad z_2 = E_2 e^{st} \tag{16}$$

leads to the corresponding characteristic equation:

$$[M_2 s^2 + M_f(s-j\lambda\omega_R)^2 + D(s-j\lambda\omega_R) + K_0+K_3](K_1+K_2+D_s s+M_1 s^2) + K_2(K_1+D_s s+M_1 s^2) = 0 \tag{17}$$

where s is the system eigenvalue, and E_1, E_2 are constants of integration. The equation (17) can easily be solved numerically. An example is presented in Figure 6. The eigenvalues are given as functions of rotative speed ω_R.

After computing several examples, it has been noticed that the modal mass M_2 and the fluid inertia M_f, when not exceeding certain "critical" values, have very little effect on the eigenvalues. It has also been noticed that one of the eigenvalues has always the imaginary part proportional to the rotative speed ω_R, when the latter is low, and that it tends to the constant value corresponding to the rotor natural frequency $\sqrt{(K_1+K_2)/M_1}$ when ω_R increases. The corresponding imaginary part of this eigenvalue crosses zero at a specific rotative speed. That is, after this specific speed, the pure rotational motion of the rotor becomes unstable.

These observations led to an important conclusion about the character of the system eigenvalues, and to approximate eigenvalue formulas.

The approximate values of three eigenvalues, i.e., three solutions of equation (17) are as follows (obtained from entensive parametric analysis of numerical solutions to eq. (17)):

$$s_1 \approx -\frac{K_0+K_3}{D} - \frac{K_2(K_1-M_1\lambda^2\omega_R^2)}{D(K_1+K_2-M_1\lambda^2\omega_R^2)} + j\lambda\omega_R \tag{18}$$

$$s_{2,3} \approx \pm j\sqrt{R_1 - jR_2} = (-\sqrt{-R_1+\sqrt{R_1^2+R_2^2}} \pm j\sqrt{R_1+\sqrt{R_1^2+R_2^2}})/\sqrt{2} \qquad (19)$$

where $R_1 \approx \frac{K_1+K_2}{M_1} - K_2^2(K_0+K_3)/R_3$, $R_2 \approx -K_2^2 D(\sqrt{\frac{K_1+K_2}{M_1}}-\lambda\omega_R)/R_3$

$$R_3 = \{[K_0+K_3-M_2(K_1+K_2)/M_1 - M_f(\sqrt{(K_1+K_2)/M_1}-\lambda\omega_R)^2]^2 + D^2(\sqrt{\frac{K_1+K_2}{M_1}}-\lambda\omega_R)^2\}M_1$$

The formulas (18), (19) give approximate eigenvalues of the rotor/bearing model (4), (5). The imaginary parts of the eigenvalues (18) and (19) represent natural frequencies. The first natural frequency, Im (s_1) is close to $\lambda\omega_R$. The second natural frequency, Im $(s_{2,3})$ is close to the shaft natural frequency $\pm\sqrt{(K_1+K_2)/M_1}$. Stronger coupling (high K_2) causes more significant divergence from these "uncoupled" natural frequencies of the system.

The real part of the eigenvalue (18) predicts the threshold of stability: For

$$\omega_R \lesssim \frac{1}{\lambda}\sqrt{\frac{K_1}{M_1} + \frac{K_2(K_0+K_3-M_2K_1/M_1)}{M_1[K_2+(K_0+K_3-M_2K_1/M_1)]}} \equiv \omega_R^{(ST)} \qquad (20)$$

the rotor pure rotative motion is stable. For $\omega_R > \omega_R^{(ST)}$ the pure rotational motion becomes unstable. The first term under the radical (20), mainly K_1/M_1, is definitely dominant. The second term contains two stiffnesses in sequence, K_2 and $(K_0+K_3-M_2K_1/M_1)$. Usually the stiffnesses K_0 and K_3 are small, mass M_2 is also small. Connection in sequence with K_2 (independently of value K_2) makes the total smaller than $K_0+K_3-M_2K_1/M_1$. It is reasonable, therefore, to reduce the expression for the rotor/bearing system stability threshold to

$$\omega_R^{(ST)} \approx \frac{1}{\lambda}\sqrt{\frac{K_1}{M_1}} \qquad (21)$$

For the unstable conditions the vibration amplitude increases exponentially in time and eventually bearing nonlinear forces become significant causing final limitation and stabilization of the vibration amplitude.

The experimental results entirely confirm this result. An increase of the stiffness K_1 (disk mounted on the shaft moved toward the rigid antifriction bearing) causes a significant increase of the system threshold of stability [17].

7. STABILITY OF THE SYNCHRONOUS SOLUTION

The stability of the synchronous vibrations (6) will be analyzed by applying the classical perturbation method [16]. Introducing the variational real variables $w_1(t)$, $w_2(t)$ (amplitude perturbation) according to the relation

$$z_1 = [A_1+w_1(t)]e^{j(\omega_R t+\alpha_1)} \quad , \quad z_2 = [A_2+w_2(t)]e^{j(\omega_R t+\alpha_2)} \qquad (22)$$

the linearized variational equations are obtained by substituting into equations (4) and (5).

$$M_1(\ddot{w}_1+2\dot{w}_1\omega_R j-\omega_R^2 w_1) + (K_1+K_2)w_1-K_2w_2e^{j(\alpha_2-\alpha_1)} = 0$$

$$M_2(\ddot{w}_2+2\dot{w}_2\omega_R j-\omega_R^2 w_2) + M_f[\ddot{w}_2+2j\omega_R\dot{w}_2(1-\lambda)-\omega_R^2 w_2(1-\lambda)^2] +$$

$$+ [D+\psi_2(A_2)]\,[\dot{w}_2+j\omega_R w_2(1-\lambda)] + \frac{d\psi_2(A_2)}{dA_2}\,w_2A_2j\omega_R(1-\lambda) + \tag{23}$$

$$+ [K_0+\psi_1(A_2)]\,w_2 + \frac{d\psi_1(A_2)}{dA_2}\,w_2A_2 + (K_2+K_3)\,w_2 - K_2w_1e^{j(\alpha_1-\alpha_2)} = 0$$

The solution of the variational equations (23) has the following form

$$w_1 = E_1e^{(st-j\omega_R t-j\alpha_1)} \quad , \quad w_2 = E_2e^{(st-j\omega_R t-j\alpha_2)} \tag{24}$$

where s is the eigenvalue and E_1, E_2 are constants of integration. By introducing (24) into (23), the characteristic equation is obtained:

$$[M_2s^2+M_f(s-j\lambda\omega_R)^2 + (D+\psi_2)(s-j\lambda\omega_R) + \psi_2'A_2j\omega_R(1-\lambda) +$$

$$+ K_0+\psi_1+\psi_1'A_2+K_3](K_1+K_2+D_ss+M_1s^2) + K_2(K_1+D_ss+M_1s^2) = 0 \tag{25}$$

where ψ_1 and ψ_2 are functions of A_2 and $\psi_{1,2}' = \frac{d\psi_{1,2}(A_2)}{dA_2}$.

Stability of the synchronous solution (6) is assured if all eigenvalues of the equations (23) have non-positive real parts.

The characteristic equation (25) differs from the characteristic equation (17) by the nonlinear terms which cause an apparent increase of the bearing radial damping, "cross stiffness" effect, and radial stiffness. The threshold of stability calculated the same way as previously, has now the following form (M_2 is neglected):

$$\omega_R^{(ST)} \equiv \frac{1}{\lambda\sqrt{M_1}[1+\chi(A_2)]}\sqrt{K_1 + \frac{K_2(K_0+K_3+\psi_1+\psi_1'A_2)}{K_2+K_0+K_3+\psi_1+\psi_1'A_2}} \tag{26}$$

where $\chi(A_2) = -\psi_2'A_2(1/\lambda-1)/(D+\psi_2)$. (27)

With increasing eccentricity A_2 an apparent decrease of the average swirling ratio λ is noticed, as $\chi(A_2)$ has a negative sign.

More interesting is, however, the modification of the instability threshold due to increase of stiffness from (K_0+K_3) in (20) to $(K_0+K_3+\psi_1+\psi_1'A_2)$ in (26). The last expression includes the amplitude of synchronous vibration A_2 which is a function of rotative speed ω_R. Following (20) and (26), the criterion of stability can be written in the form:

$$\lambda\sqrt{M_1}[1+\chi(A_2)]\omega_R < \sqrt{K_1 + \frac{K_2(K_0+K_3+\psi_1+\psi_1'A_2)}{K_2+K_0+K_3+\psi_1+\psi_1'A_2}} = \sqrt{K_1 + \frac{K_2\psi}{K_2+\psi}} \tag{28}$$

and solved graphically (Fig. 7). The graphical solution is very effective in showing qualitative features of the rotor dynamic behavior. Having the amplitude/rotative speed relationship from equation (8) or (13) (lower graph of Fig. 7) and having the plot of the radical (28) versus amplitude A_2 which includes the nonlinear function ψ_1 of A_2 (left-hand side graph), the graph of the radical from the right-hand side of the inequality (28) versus rotative speed ω_R can be built up as the small arrows indicate (right side plot). The left-hand side of the inequality (28) versus ω_R is a straight line $\lambda\omega_R\sqrt{M_1}$ slightly modified by the factor $\chi(A_2)$. The regions of stability are found at intersections of the corresponding plots on the

upper right-hand side graph. It clearly shows that the synchronous solution is stable for rotative speeds below the first threshold of stability, which differs very little from the stability threshold (21), and that they are stable in the resonant speed region.

It is easily noticed that higher unbalance will increase stability region for the synchronous vibrations around the resonant speed $\sqrt{(K_1+K_2)/M_1}$ (Fig. 8).

The series of experiments with a balanced and unbalanced rotor confirm this analytical prediction; higher unbalance causes wider interval of rotative speeds where synchronous vibrations are stable (Figs. 9 through 11).

8. ROTOR SELF-EXCITED VIBRATIONS: OIL WHIRL AND OIL WHIP

For the case of the absence of imbalance, the equations (4), (5) have a particular solution describing self-excited vibrations (oil whirl and oil whip).

$$z_1 = G_1 e^{j(\omega t+\beta)} \quad , \quad z_2 = G_2 e^{j\omega t} \tag{29}$$

where G_1, G_2 are corresponding constant amplitudes, β is the relative phase angle, and ω is the self-excited vibration frequency.

By introducing (29) into (4) and (5), the algebraic equations for calculating G_1, G_2, β, and ω are obtained:

$$\{-M_2\omega^2-M_f(\omega-\lambda\omega_R)^2 + j[D+\psi_2(G_2)](\omega-\lambda\omega_R) + K_0+\psi_1(G_2) + K_3](K_1+K_2-M_1\omega^2+D_s j\omega) + \\ + K_2(K_1+D_s j\omega-M_1\omega^2) = 0 \tag{30}$$

$$G_1 = \frac{K_2 G_2}{\sqrt{(K_1+K_2-M_1\omega^2) + D_s^2\omega^2}} \quad , \quad \beta = \arctan \frac{D_s\omega}{M_1\omega^2-K_1-K_2} \tag{31}$$

The real and imaginary parts of the equation (30) provide relationships for obtaining G_2 and ω, for each case of the nonlinear functions $\psi_1(G_2)$ and $\psi_2(G_2)$:

$$\psi_1(G_2) = M_2\omega^2+M_f(\omega-\lambda\omega_R)^2-K_0-K_3-K_2 \frac{(K_1+K_2-M_1\omega^2)(K_1-M_1\omega^2) + D_s^2\omega^2}{(K_1+K_2-M_1\omega^2)^2 + D_s^2\omega^2} \equiv \phi_1(\omega) \tag{32}$$

$$\psi_2(G_2) = -D - \frac{K_2^2 D_s\omega}{(\omega-\lambda\omega_R)[(K_1+K_2-M_1\omega^2)^2 + D_s^2\omega^2]} \equiv \phi_2(\omega) \tag{33}$$

The frequency ω is yielded from the equation

$$\psi_2\{\psi_1^{-1}[\phi_1(\omega)]\} = \phi_2(\omega) \tag{34}$$

where ψ_1^{-1} is the inverse function (32); $G_2 = \psi_1^{-1}[\phi_1(\omega)]$.

For example, in case of the "parabolic" nonlinear functions (2) and small damping D_s

the frequency equation (34) has the following form:

$$(K_1+K_2-M_1\omega^2)(\omega-\lambda\omega_R)\{(K_1+K_2-M_1\omega^2)[\frac{B_2}{B_1}(K_0+K_3-M_2\omega^2-M_f(\omega-\lambda\omega_R)^2)-D] + \\ + \frac{B_2}{B_1}K_2(K_1-M_1\omega^2)\} \approx D_s\omega K_2^2 \approx 0 \tag{35}$$

It yields immediately three important real solutions for the frequency:

$$\omega_1 \approx \lambda\omega_R \tag{36}$$

$$\omega_{2,3} \approx \pm\sqrt{(K_1+K_2)/M_1 + D_sB_1/[M_1B_2(1-\lambda\omega_R/\sqrt{(K_1+K_2)/M_1})]} \approx \pm\sqrt{(K_1+K_2)/M_1} \tag{37}$$

which are close to the linear rotor/bearing system "whirl" and "whip" natural frequencies at the threshold of stability (21). The remaining solutions can be also easily obtained from equation (35). For the small shaft damping D_s the similar consideration can be extended to any case of nonlinear functions ψ_1, ψ_2: in (35) the ratio B_2/B_1 should be replaced by the ratio $\psi_2(G_2)/\psi_1(G_2)$. Three frequency solutions (36), (37) exist, therefore, independently of nonlinearities and independently of journal mass and fluid inertia.

The corresponding amplitude G_2 of the self-excited vibrations can be calculated from (32). For example, the "parabolic" nonlinearity (2) yields:

Whirl amplitude: $$G_2\Big|_{\omega=\lambda\omega_R} \approx \frac{1}{B_1}\sqrt{M_2\lambda^2\omega_R^2-K_0-K_3-K_2\,\frac{K_1-M_1\lambda^2\omega_R^2}{K_1+K_2-M_1\lambda^2\omega_R^2}} \tag{38}$$

Whip amplitude: $$G_2\Big|_{\omega=\sqrt{(K_1+K_2)/M}} \approx \frac{1}{B_1}\sqrt{M_2(K_1+K_2)/M_1+M_f(\sqrt{(K_1+K_2)/M_1}-\lambda\omega_R)^2 - K_0-K_2-K_3} \tag{39}$$

The expression under the radical (38) should be positive, therefore, the self-excited vibrations with the whirl amplitude (38) exist only for the limited range of the rotative speed (M_2 neglected):

$$\frac{1}{\lambda}\sqrt{\frac{K_1}{M_1}+\frac{K_2(K_0+K_3)}{M_1(K_0+K_2+K_3)}} \lesssim \omega_R \lesssim \sqrt{(K_1+K_2)/M_1}/\lambda \tag{40}$$

The left-hand side of the inequality (40) represents the threshold of stability (20), the right-hand side term separates the whirl from the whip.

The similar reason causes that the self-excited vibrations with the whip amplitude (39) exist for the following rotative speed range:

$$\omega_R \gtrsim \frac{1}{\lambda}\sqrt{\frac{K_1+K_2}{M_1}} + \frac{1}{\lambda}\sqrt{[K_0+K_2+K_3-(K_1+K_2)M_2/M_1]/M_f} \tag{41}$$

From equations (31) and (32) the corresponding whirl and whip amplitudes and phases of the rotor can be obtained. For example for whip frequency (37), in case of "parabolic" nonlinearities (2) they are as follows:

$$G_1 = G_2\Big|_{\omega=\sqrt{(K_1+K_2)/M}} \frac{K_2}{D_s\sqrt{(K_1+K_2)/M_1}\ \sqrt{B_1^2/[B_2(\sqrt{(K_1+K_2)/M_1}-\lambda\omega_R)]^2+1}} \tag{42}$$

$$\beta = \arctan\left[B_2(\sqrt{(K_1+K_2)/M_1}-\lambda\omega_R)/B_1\right] \tag{43}$$

During whip, the shaft vibrates at its resonant conditions, the whip amplitude is controlled mainly by the shaft damping D_s and the nonlinear fluid forces.

The phase between the rotor and journal at whip vibrations is controlled by nonlinear forces in the bearing. It was experimentally verified that during both oil whirl and oil whip, the rotor and journal vibrate nearly in phase (Fig. 12). This may serve as an indication concerning the values of nonlinear forces ψ_1 and ψ_2.

9. DISCUSSION OF RESULTS

In this paper, a simple mathematical model of a symmetric shaft rotating in one rigid and one 360° lubricated bearing is proposed. The model yields results which stand in very good agreement with the experimentally observed rotor dynamic phenomena concerning stability, thresholds, and the self-excited vibrations known as oil whirl and oil whip.

The rotor in the model is represented by the generalized (modal) parameters of its first bending mode. These parameters can be analytically obtained by applying any classical method of modal reduction. The fluid force acting at the journal is represented in the model by the nonlinear expression based on rotating character of this force. The latter approach yields the bearing coefficients in an "interrelated" form: the tangential ("cross") stiffness is a product of the relative velocity and radial damping, the tangential damping results from Coriolis acceleration, the radial stiffness is reduced due to centripetal acceleration and fluid inertia.

The fluid nonlinear force is introduced in a very general form, where the nonlinearity is related to the journal radial displacement (eccentricity in the journal bearing). The nonlinear character of the fluid stiffness force and especially fluid damping force is well known. This nonlinearity has a "hard" character: the forces increase with eccentricity. Actually they grow to infinity when the journal touches the bearing wall. Since, in this paper, low eccentricity ratios were considered only (to justify the symmetric character of the rotor model), an example of the fluid nonlinear forces was discussed: the first terms of the Fourier expansion of any nonlinear function representing the fluid force.*

The results obtained from the analysis of the rotor model and concerning the rotor, synchronous vibrations due to imbalance, and self-excited vibrations known as "oil whirl" and "oil whip" very well reflect the observed rotor dynamical behavior.

The classical eigenvalue problem yields three important eigenvalues of the rotor/bearing system. The first eigenvalue has the imaginary part (natural frequency) close to $\lambda\omega_R$ and corresponds to oil whirl frequency. The real part of this eigen-

value predicts the threshold of stability (the rotative speed at which the pure rotational motion or 1× synchronous vibrations of an unbalanced rotor become unstable). This threshold of stability is determined by the rotor mass and its partial stiffness, as well as the oil average swirling ratio ($\omega_{R}^{(ST)} \approx \sqrt{K_1/M_1}/\lambda$ expression (21)). The latter result was noticed in the fifties by Poritsky [18] and discussed by Boeker and Sternlicht [19]. Since then, this seems to have been forgotten for 30 years.

The second and third eigenvalue of the rotor/bearing system have the imaginary part close to the rotor natural frequency ($\pm\sqrt{(K_1+K_2)/M_1}$) of the first bending mode. The latter is referred to as "whip frequency".

The model yields the self-excited vibrations (known as oil whirl and oil whip) as a particular solution. The frequencies of oil whirl and oil whip are very close to the natural frequencies of the linear system. The model permits evaluation of the amplitudes and relative, journal/disk phase angles of these self-excited vibrations.

The most important and new (to the author's knowledge) result presented in this paper concerns the analytical evaluation of the stability of the synchronous vibrations of the rotor and relationship between the width of the stability region and the amount of the rotor imbalance. This result is yielded from the classical investigation of stability through equations in variations. The bearing nonlinear force, increasing with rotor radial deflection causes an increase of the journal supporting radial stiffness force which is directly related to the actual synchronous vibration amplitude. The increased radial stiffness affects the threshold of stability. The synchronous vibration amplitude varies with the rotative speed, and in the first balance resonance region of speeds the effect of stable synchronous vibrations is observed. Two additional thresholds of stability are noted. The width of this region depends directly on the amount of imbalance in the rotating system. A simple graphical method (Figs. 7 and 8) explains qualitatively this feature. The expressions (26) and (28) give the analytical relationships for these additional thresholds of stability.

In the rotor/bearing system analysis, as well as in experimental testing, rather small effect of the bearing fluid inertia has been noted. The fluid inertia has a negligible influence on the synchronous vibrations, thresholds of stability, natural frequencies, and frequencies of the self-excited vibrations. The journal generalized (modal) mass is also usually relatively small. These aspects led to the conclusion regarding further simplifications of the rotor/bearing model to the one and a half degree of freedom system. The fluid radial damping force which is proportional to the relative journal velocity is definitely dominant fluid force in the bearing, and it determines the order of the equation (5), as the forces of inertia M_f and M_2 are negligible.

There is still no clear picture of what affects the fluid average swirling ratio λ. It has been assumed in this paper that λ is constant. However, during experimental testing some variations of value of λ have been noticed. This aspect is being studied and requires further investigation.

---

* Fluid force is often modeled proportional to $(1-e^2)^{-n}$, where e is the eccentricity ratio (journal radial displacement $|z_2|$ to radial clearance), n is a number (usually 1/2, 1, 3/2, 2, 5/2, or 3). In the first approximation $(1-e^2)^{-n} \approx 1 + 2ne^2$, which in turn, is proportional to the example forces (2) considered in this paper.

SYMBOLS

A_1, A_2	Amplitudes of synchronous vibrations of the rotor and journal respectively
B_1, B_2	Coefficients of bearing nonlinear "parabolic" force (2)
D, K_0, M_f	Bearing fluid radial damping, stiffness, and inertia coefficients
D_s	Shaft external damping coefficient
E_1, E_2	Constants of integration
F	Bearing fluid force
G_1, G_2	Amplitudes of the rotor and journal self-excited vibrations
$j = \sqrt{-1}$	
K_1, K_2, K_3	Rotor modal stiffness coefficients
m, r	Mass and radius of imbalance respectively
M_1, M_2	Rotor and journal modal masses respectively
s, s_1, s_2, s_3	Eigenvalues
$w_1(t)$, $w_2(t)$	Variational variables for the synchronous vibration/stability investigation
$z=x+jy$, $z_2=x_2+jy_2$	Journal radial displacement x-horizontal, y-vertical (fixed coordinates)
$z_1 = x_1+jy_1$	Rotor radial displacement (x_1-horizontal, y_1-vertical)
$z_r = x_r+jy_r$	Journal radial displacement (rotating coordinates)
α_1, α_2	Rotor and journal phase of the synchronous vibrations
β	Phase of rotor/journal self-excited vibrations
λ	Fluid average swirling ratio
ψ_1, ψ_2	Bearing fluid nonlinear functions of journal radial displacement
ψ_1', ψ_2'	Derivatives of ψ_1, ψ_2 in respect to radial displacement correspondingly
ω	Circular frequency of the rotor self-excited vibrations
ω_R	Rotative speed
$\omega_R^{(ST)}$	Threshold of stability (rotative speed).

REFERENCES

1. Symposium of Dynamics of Rotors IUTAM. Lyngby, Denmark, 1974. Proceedings, Springer Verlag, 1975.
2. Vibrations in Rotating Machinery. Proceedings of the Conference, University of Cambridge, UK, 1976.
3. Rotordynamic Instability Problems in High Performance Turbomachinery. NASA CP-2133, Texas A&M University Workshop, 1980.
4. Vibrations in Rotating Machinery. Proceedings of the Conference, University of Cambridge, UK, 1980.
5. Rotordynamic Instability Problems in High Performance Turbomachinery. NASA CP-2250, Texas A&M University Workshop, 1982.
6. Rotordynamic Instability Problems in High Performance Turbomachinery. Texas A&M University Workshop, 1984.
7. Vibrations in Rotating Machinery. Proceedings of the Third International Conference, York, UK, 1984.
8. Bolotin, V.V.: The Dynamic Stability of Elastic Systems (translated from Russian), Holden-Day Inc., San Francisco, 1964.

9. Humphris, R.R., Gunter, E.J.: The Influence of Rotor Characteristics in Oil Whirl. Rotor Dynamics Laboratory, University of Virginia, Charlottesville, VA, June 1983.
10. Muszynska, A.: Rotor Instability. Senior Mechanical Engineering Seminar, Bently Nevada Corporation, Carson City, Nevada, June 1984.
11. Black, H.F.: Effects of Hydraulic Forces in Annular Pressure Seals on the Vibrations of Centrifugal Pump Rotors. Journal of Mechanical Engineering Science, Vol. II, No. 2, 1969.
12. Black, H.F., Jensen, D.N.: Dynamic Hybrid Bearing Characteristics of Annular Controlled Leakage Seals. Proceedings Journal of Mechanical Engineering, Vol. 184, 1970.
13. Bently, D.E., Muszynska, A.: Perturbation Tests of Bearing/Seal for Evaluation of Dynamic Coefficients. Symposium on Rotor Dynamical Instability, Summer Annual Conference of the ASME Applied Mechanics Division, Houston, TX, June 1983.
14. Ambrosch, F., Schwaebel, R.: Method of and Device for Avoiding Rotor Instabiltiy to Enhance Dynamic Power Limit of Turbines and Compressors. United States Patent, #4,273,510, June 1981.
15. Miller, E.H.: Rotor Stabilizing Labyrinth Seal for Steam Turbines. United States Patent #4,420,161, Dec. 1983.
16. Minorsky, N.: Introduction to Nonlinear Mechanics. J. W. Edwards, Ann Arbor, 1947.
17. Bently, D.E., Muszynska, A.: Perturbation Study of a Rotor/Bearing System: Identification of the Oil Whirl and Oil Whip Resonances. Tenth Biennial ASME Conference on Mechanical Vibration and Noise, Cincinnati, Ohio, September 1985.
18. Poritsky, H.: Contribution to the Theory of Oil Whip. Trans. ASME v. 75, 1953.
19. Boeker, G. F., Sternlicht, B.: Investigation of Translatory Fluid Whirl in Vertical Machines. Trans. ASME, January 1956.

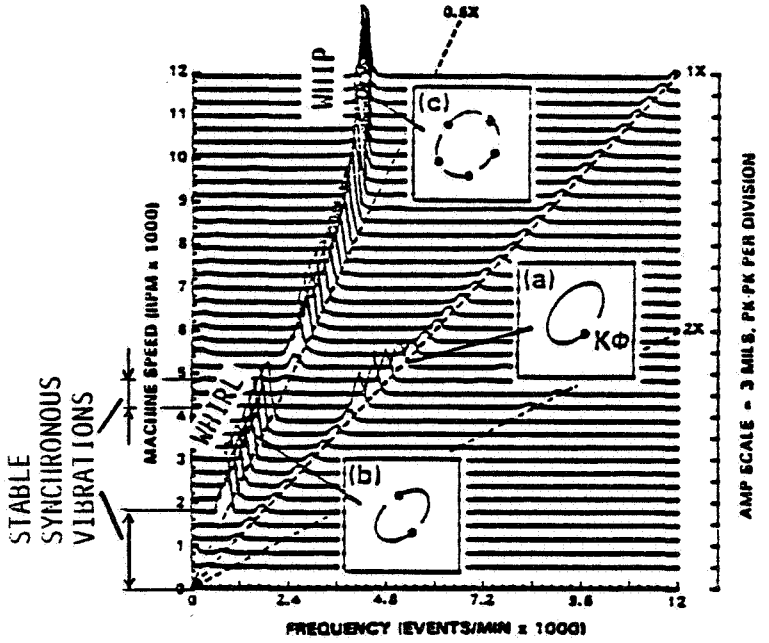

Figure 1. - Cascade spectrum of rotor vibrational response measured at oil bearing. Spectrum indicates regions of synchronous (1X) vibrations due to unbalance, oil whirl (≈1/2X), and oil whip with constant frequency close to first balance resonance (slightly lower). (a) Orbit display of synchronous vibrations, (b) oil whirl orbit, (c) oil whip orbit (Kφ - keyphasor pulse indicating relationship with rotative speed frequency).

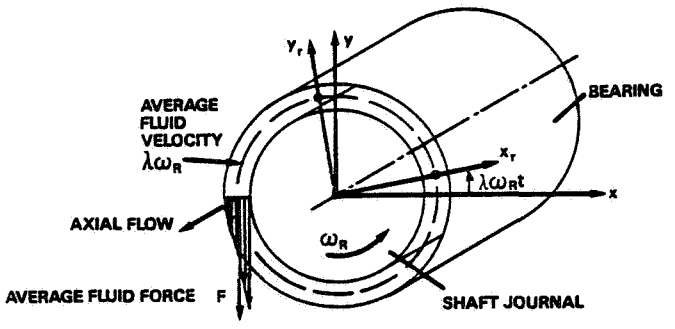

Figure 2. - Bearing mode: Fluid force rotating with angular velocity $\lambda\omega_R$.

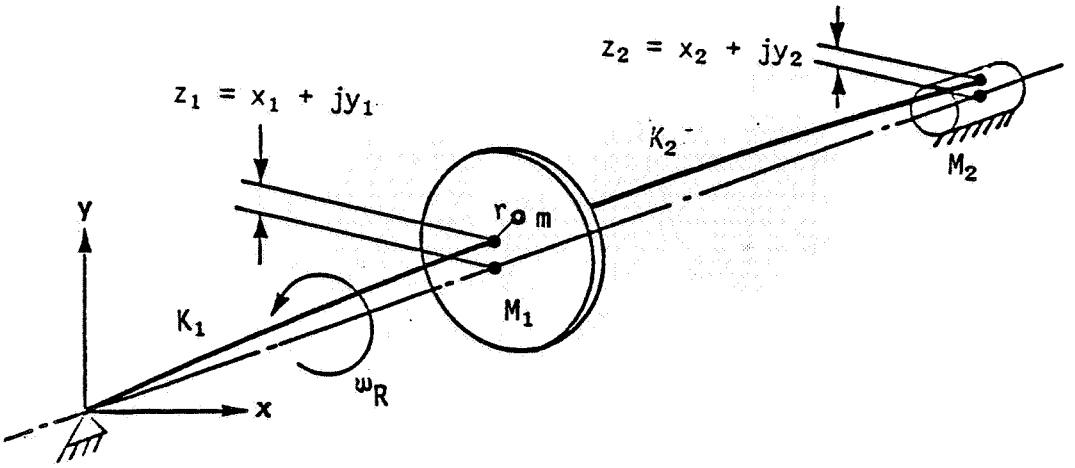

Figure 3. - Model of symmetric rotor in one antifriction and one oil bearing.

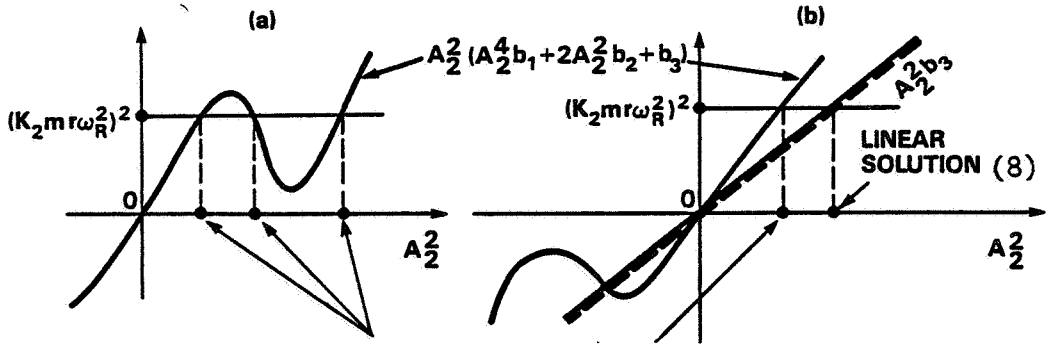

(a) Case $2b_2 < -\sqrt{3b_1 b_3}$: three amplitudes A_2 yielded.

(b) Case $2b_2 \geq -\sqrt{3b_1 b_3}$: one amplitude A_2 exists.

Figure 4. - Graphical solution of equation (13) (notation: $b_1 = h_6^2 + h_7^2$, $b_2 = h_2 h_6 + h_3 h_7$, $b_3 = h_2^2 + h_3^2$).

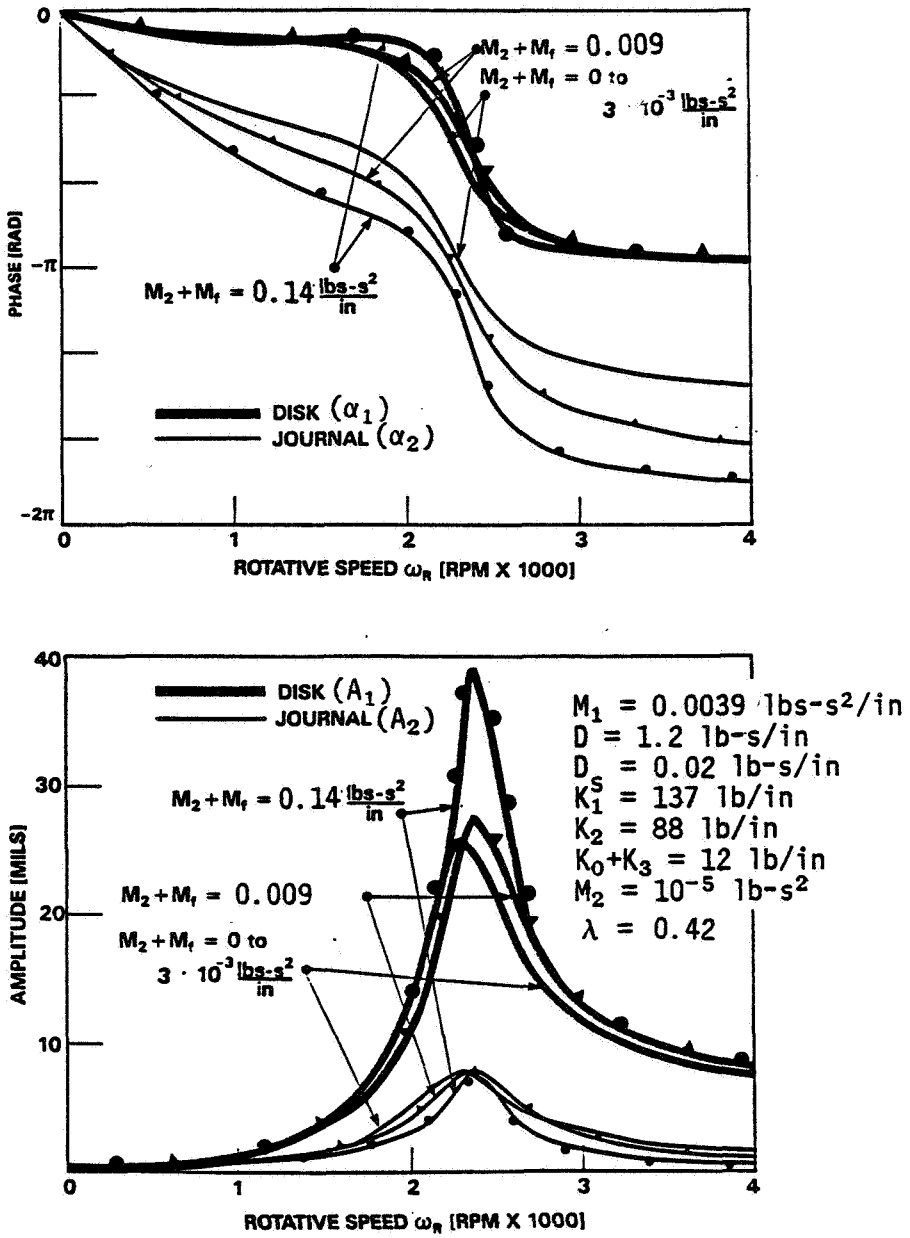

Figure 5. - Phase and amplitude of rotor and journal synchronous vibrations (6) versus rotative speed. Note a significant insensitivity to fluid inertia and journal generalized mass M_2.

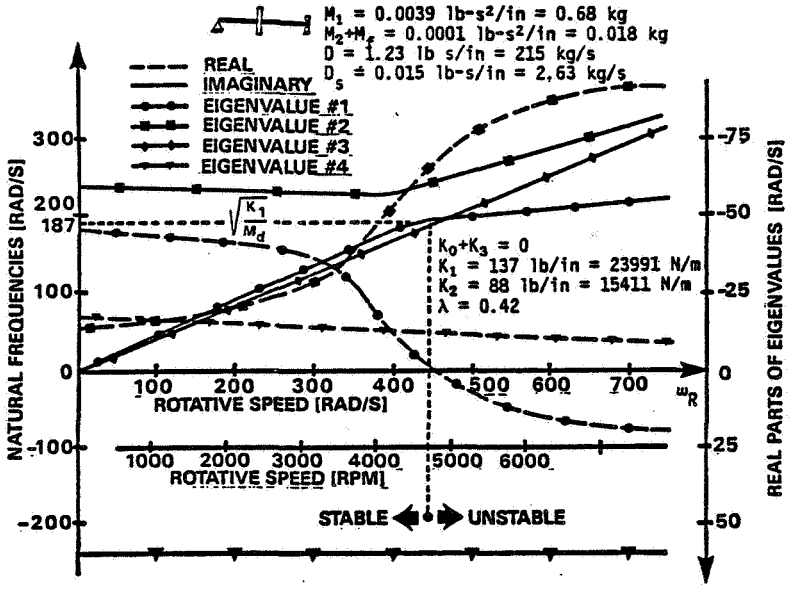

Figure 6. - Eigenvalues of rotor/bearing system (eigenvalue "3" has a high-value negative real part, not shown in graph).

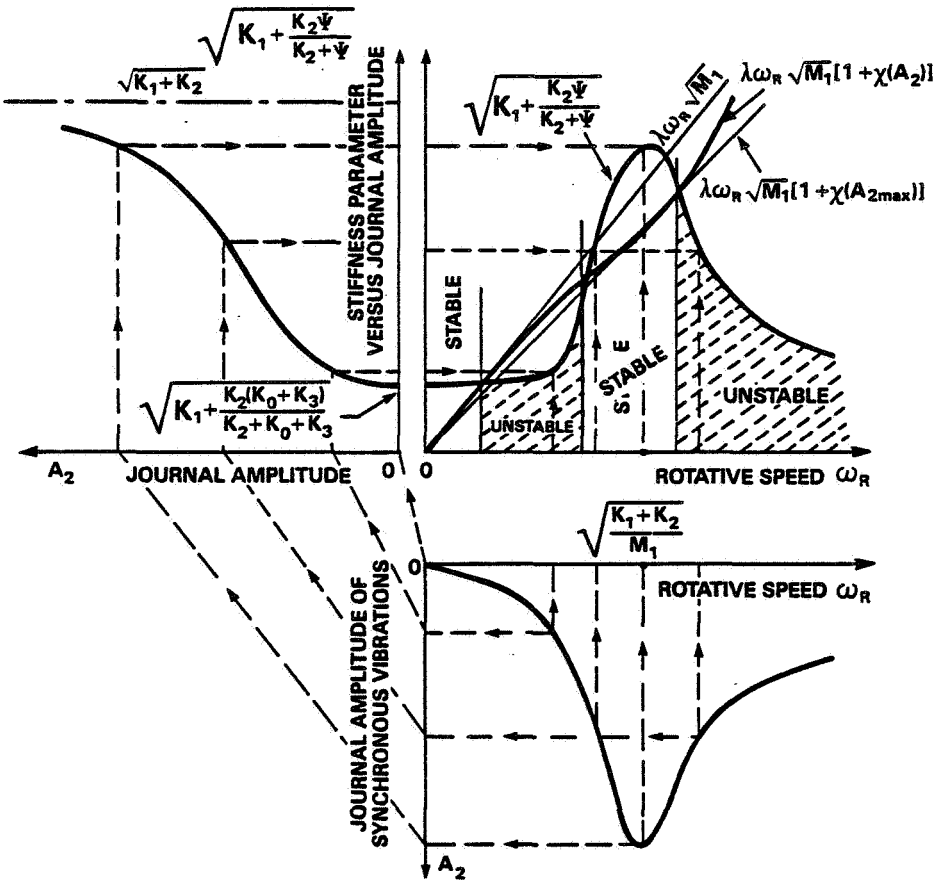

Figure 7. - Stability chart for rotor synchronous vibrations due to unbalance. Graphical solution of inequality (48). [Notation: $\psi = K_0 + K_3 + \psi_1(A_2) + A_2\psi_1'(A_2)$.]

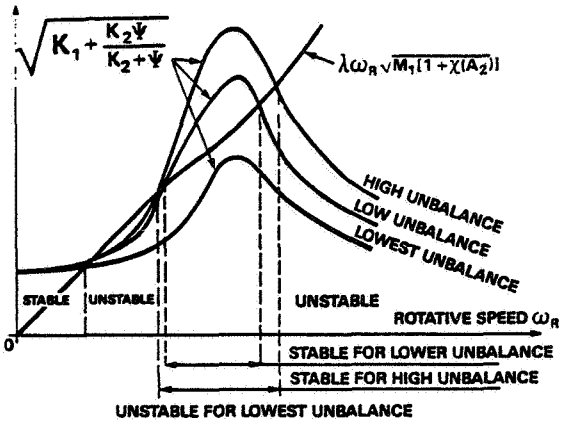

Figure 8. - Modification of synchronous vibration stability regions by unbalance (ψ same as in fig. 7).

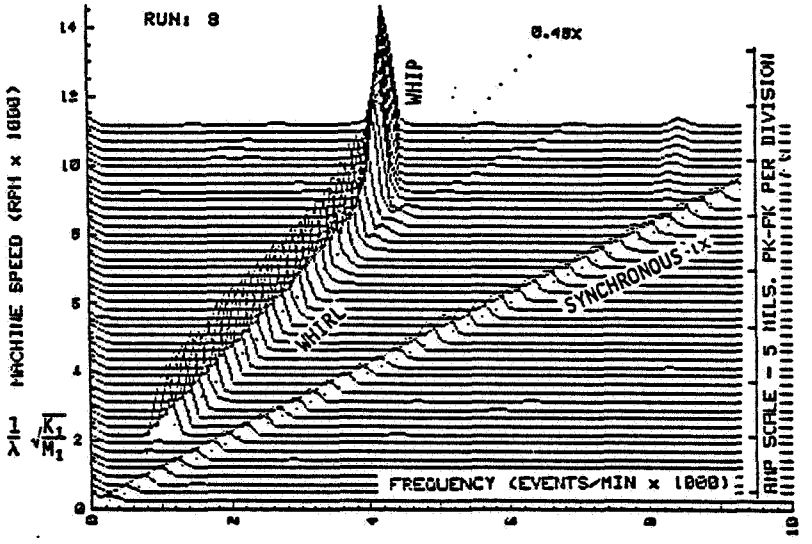

Figure 9. - Cascade spectrum of rotor with residual unbalance. Vertical response measured at journal. Synchronous vibrations unstable for rotative speed higher then ~2100 rpm.

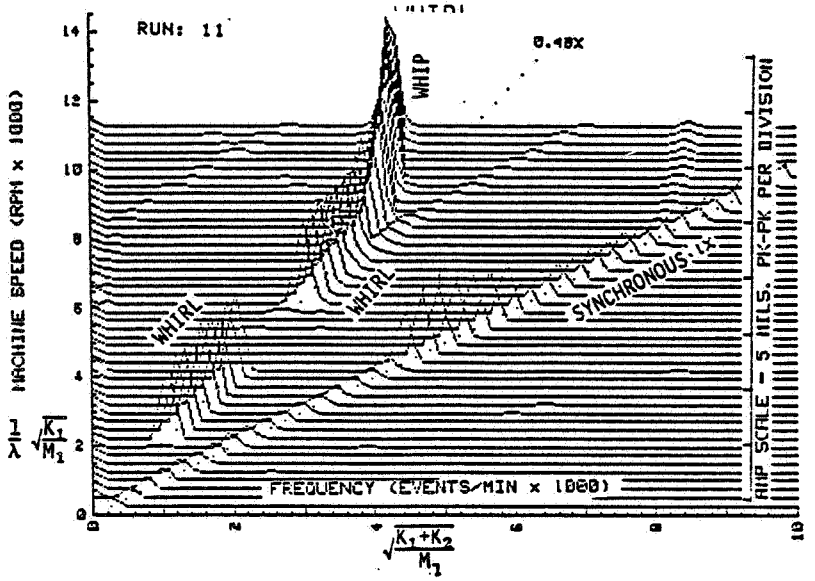

Figure 10. - Cascade spectrum of rotor with 1 g x 1.2 in. of imbalance. Vertical response of journal. Synchronous vibrations stable for rotative speed lower than ~2100 rpm and in resonance region: from ~4200 to ~4900 rpm.

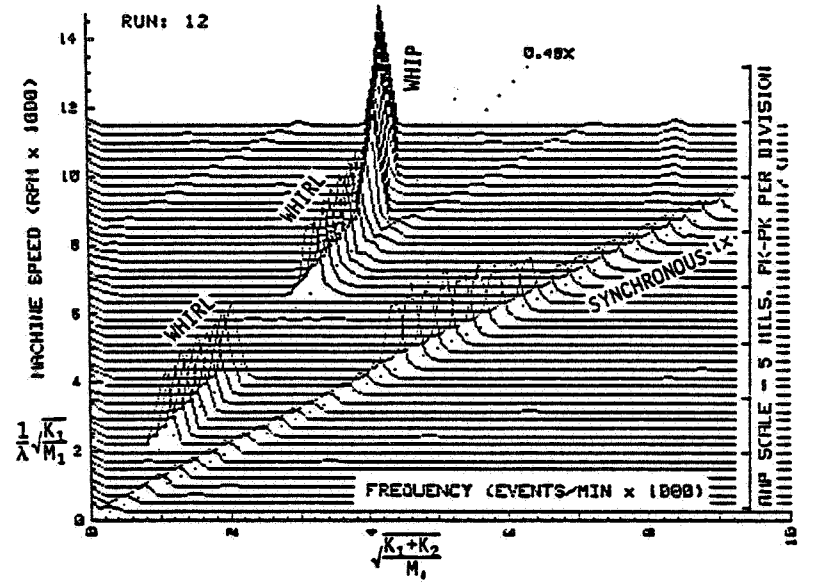

Figure 11. - Cascade spectrum of rotor with 1.2 g x 1.2 in. of imbalance. Vertical response of journal. Synchronous vibrations stable for rotative speed lower than ~2100 rpm and in wider resonance region: from ~4100 to ~5200 rpm.

Figure 12. - Vertical transducer signals of journal and rotor vibrations during oil whip. Oscilloscope display in XY mode indicates nearly in-phase vibrations.